J Electr Eng Technol Vol. 8, No. 4: 938-944, 2013
http://dx.doi.org/10.5370/JEET.2013.8.4.938

ISSN(Print) 1975-0102
ISSN(Online) 2093-7423

Suppression of Shaft Voltage by Rotor and Magnet Shape Design of IPM-Type High Voltage Motor

Kyung-Tae Kim*, Sang-Hoon Cha, Jin Hur*, Jae-Sun Shim*** and Byeong-Woo Kim†**

Abstract – In this paper, we propose a method for suppressing shaft voltage by modifying the shape of the rotor and the permanent magnets in interior permanent magnet-type-high-voltage motors. Shaft voltage, which is induced by parasitic components and the leakage flux in motor-driven systems, adversely affects their bearings. In order to minimize shaft voltage, we designed a magnet re-arrangement and rotor re-structuring of the motor. The shaft voltage suppression effect of the designed model was confirmed experimentally and by comparative finite element analysis.

Keywords: Shaft voltage, Bearing fault, Common mode voltage, Parasitic parameter, V-shaped motor, Interior permanent magnet motor

1. Introduction

The electric vehicle is used many motors. Also, the heavily equipped vehicle is used high-voltage motor. So, shaft voltage has become a serious problem in interior permanent magnet (IPM)-type motors. In addition, the lifetime and the reliability of such motors are greatly reduced by bearing faults, which are caused by the induced voltage on the shaft's surface. These bearing faults create motor vibration and noise, which are the main causes of motor faults. There are four causes of shaft voltage in a motor: electrostatic shaft voltage, magnetic unbalanced shaft voltage, electromagnetic shaft voltage and shaft voltage from the external power supply. Among these four causes, electromagnetic shaft voltage and external power-supply are the primary causes of shaft voltage. Magnetic unbalanced shaft voltage is caused by modification of the stator core and eccentricity between the stator and rotor. Shaft voltage from the external power supply is caused by the common mode voltage, which is due to a parasitic component as well as leakage flux from the high input voltage and high frequency of the inverter. Shaft voltage can be suppressed with insulated bearings, shaft grounding rings, grounding brushes, Faraday shields, conductive grease, insulated rotors, etc. [1, 2]. There are many ways to suppress shaft voltage, but they cannot be used in special circumstances. For example, a motor with the fragile insulating material cannot be high- temperature parts and cannot be used in the deep sea because of high hydraulic pressure.

† Corresponding Author: Dept. of Electrical Engineering, Ulsan University, Korea. (bywokim @ulsan.ac.kr)
* Dept. of Electrical Engineering, Ulsan University, Korea. (jinhur@ulsan.ac.kr, kkt2782@nate.com)
** Korea Marine Equipment Research Institute, Korea. (sang3806@komeri.re.kr)
*** Dept. of Electrical Engineering, Kangwon National University, Korea. (namsuk6645@daum.net)
Received: May 27, 2013; Accepted: June 7, 2013

The magnetic circuit technique of modifying the permanent magnet and rotor shape in an IPM motor to suppress shaft voltage has not yet been described in detail in the literature. Therefore, in order to suppress shaft voltage, we propose an improved shape for permanent magnets that will not affect the torque characteristics.

Consequently, in this paper, we propose suppressing shaft voltage by modifying the magnet and rotor shape, taking the common mode voltage into consideration. The shaft voltage suppression in IPM-type high-voltage motors was confirmed through experiments. In addition, the proposed method was validated by the finite element method (FEM).

2. The Cause of Shaft Voltage

2.1 Electrostatic shaft voltage

An electrostatic shaft voltage is induced by friction static electricity in motor-driven systems of shaft included electrostatic capacity. This shaft voltage in motor driven-system mostly occurs in the drive belt, and is the direct current component.

2.2 Magnetic unbalanced shaft voltage

Magnetic unbalanced shaft voltage is induced by structure, material, and work deviation such as the commissure of the segmented stator core, the segment-contact of the core, transformation of the stator core and the eccentricity between the rotor and stator.

Thus, the linkage magnetic flux of the shaft occurs because by magnetic unbalance.

2.3 Shaft voltage from the external power supply

Shaft voltage from the external power supply occurs

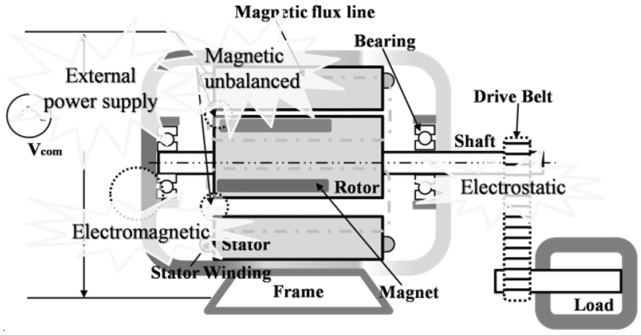

Fig. 1. The cause of shaft voltage

because of the high frequency and leakage current in the inverter. In addition, the common mode voltage has become a serious problem.

2.4 Electromagnetic shaft voltage

Electromagnetic shaft voltage occurs because of the magnetic field that rotates with the shaft, the stationary magnetic field in the case, combination with the magnetic field of the rotor and stator, and the residual magnetism of components. The magnetic-induced voltage causes vibration and instability of the rotated axis.

Fig.1 shows the causes of shaft voltage in the motor. There are four causes of shaft voltage in a motor: electrostatic shaft voltage, magnetic unbalanced shaft voltage, shaft voltage from the external power supply, and electromagnetic shaft voltage. Among these four causes, electromagnetic shaft voltage and external power-supply are the primary causes of shaft voltage. Magnetic unbalanced shaft voltage is caused by modification of the stator core and eccentricity between the stator and rotor. Shaft voltage from the external power supply is caused by the common mode voltage, which is due to a parasitic component as well as leakage flux from the high input voltage and high frequency of the inverter.

3. The Ways of Suppression of Shaft Voltage

Numerous papers have been published by both motor manufacturers and drive manufacturers in the last several years that attempt to understand the causes of shaft voltage in motors and to find a solution to eliminate electrical bearing damage. The bearing can be protected from the shaft voltage in the following ways:

3.1 Insulated bearing

Insulating material, such as a nonconductive resin or ceramic layer isolates the bearings and prevents the shaft current from discharging through them to the frame. Nonconductive ceramic ball bearings prevent the discharge of the shaft current through the bearing. As with other isolation measures, shaft current will seek an alternate path to ground possibly through equipment connected to the motor. Such Bearings are very costly and, in most cases, motors with ceramic bearings must be special ordered and so have long lead times.

3.2 Shaft grounding ring

A metal brush contacting the motor shaft is a more practical way and economical way to provide a low-impedance path to ground, especially for larger frame motors. However, these brushes pose several problems of their own.

3.3 Faraday shield

A conductive shield between the rotor and the stator inside the motor would prevent the variable frequency drive current from being induced onto the shaft by effectively blocking it with a capacitive barrier.

3.4 Insulated rotor

The rotor core increases the magnetic flux density as the back yoke of a permanent magnet. An insulation insert inside the rotor reduces shaft voltage.

There are many methods to reduce the shaft voltage, but some of these cannot be used in special cases. For example, fragile insulating materials cannot be used at extreme temperature because they are easily broken or melted. In such cases, there is no option to suppress shaft voltage by modifying the magnetic and electric circuits [1, 2].

3.5 Conductive grease

In theory, because this grease contains conductive particles, it should provide a continuous path through the bearing and so bleed off shaft voltages gradually through the bearing without causing a damaging discharge. Unfortunately, the conductive particles in these lubricants may increase mechanical wear into the bearing, rendering the lubricants ineffective and often causing premature failures. This method has been widely abandoned as a viable solution to bearing currents.

4. Calculation of the Parasitic Parameter and Shaft Voltage in a Motor Structure

When the system is operating, the parasitic component and leakage flux occur due mainly to high input voltage and the high frequency of the inverter. In order to calculate shaft voltage, the parasitic component should be calculated first. A detailed mathematical analysis will be carried out to determine the effects of these parameters on motor shaft voltage. Fig. 2 shows the structure of a high-voltage motor,

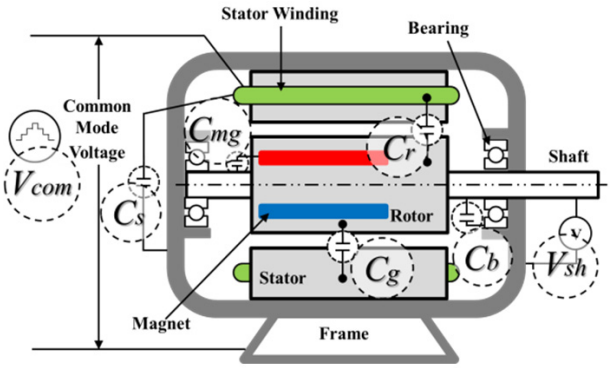

Fig. 2. Structure of IPM-type motor for capacitance

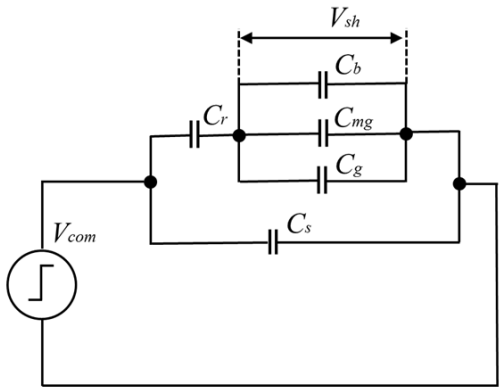

Fig. 3. Equivalent circuit

where, parasitic capacitance couplings exist between the stator winding and rotor (C_r), the stator winding and stator frame (C_s), the rotor and stator frames (C_g), the magnet capacitance (C_{mg}), ball bearing capacitance (C_b). Fig. 3 shows equivalent circuit including common mode voltage for calculating shaft voltage [3-6].

4.1 Composite capacitance between the winding and the stator core: C_s

There are 4 surfaces which surround the winding in the slot. The C_s can be calculated as follows

$$C_s = \frac{N_s \varepsilon_0 \varepsilon_{rc} (w_d + 2 \times w_f) \times L_s}{g_{in}} \tag{1}$$

where, N_S is the number of slots, w_d is the slot width, w_f is the slot height, L_S is the stator length, g_{in} is the insulation thickness, and ε_{rc} is the dielectric constant of the coil.

4.2 Composite capacitance between the winding and the rotor core: Cr

By considering the air-gap to be much smaller than the outer diameter of the rotor, a capacitance coupling between rotor and stator frame in stator slot can be calculated as follows

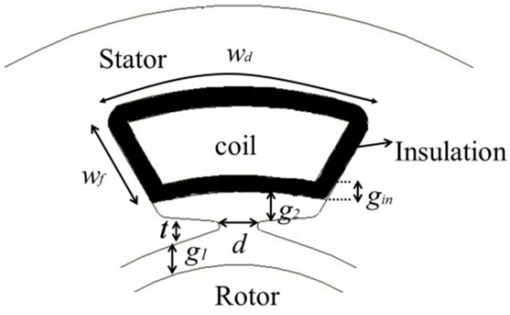

Fig. 4. The slot design factors

$$C_r = \frac{\varepsilon_0 \times N_s \times d \times L_s}{t + g_1 + g_2} \tag{2}$$

The slot design factors explain as shown in Fig. 4.

4.3 Electrostatic capacity between the stator core and the rotor core: C_g

Electrostatic capacitance of the stator and the rotor surface were measured. C_g can be calculated as follows

$$C_g = \frac{\varepsilon_0 \times \pi \times L_r}{\ln \frac{b}{a}} \tag{3}$$

where, L_r is the rotor length, a is the radius of the rotor, and b is the radius of the inside stator.

4.4 Composite capacitance between the magnet and the shaft: C_{mg}

The magnet capacitance between the rotor surface and the shaft was measured. C_{mg} can be calculated as follows

$$C_{mg} = \frac{N_m \times \varepsilon_0 \times w_m \times L_r}{d_m} \tag{4}$$

where, N_m is the number of magnets, w_m is the magnet width, and d_m is the distance between the magnet and the shaft.

4.5 Ball Bearing capacitance: C_B

The ball bearing capacitance is calculated by

$$C_B = \frac{2\pi\varepsilon_0 \varepsilon_{rb} L_b}{\ln \frac{k-m}{2j}} \tag{5}$$

where, L_b is the roller length of the bearing, k is the inner radius of the bearing outer race, m is the outer radius of the bearing inner race, j is the ball radius of the bearing, and ε_{rb}

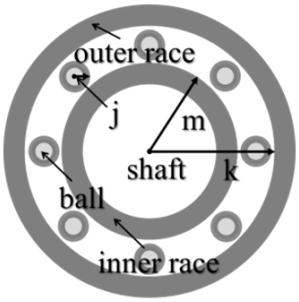

Fig. 5. The factor of ball bearing

is the dielectric constant of the coil. Fig. 5 shows the factor of ball bearings.

4.6 Common mode voltage and shaft voltage: v_{com}, V_{sh}

Eq. (6) shows common mode voltage, which is obtained by adding the three voltages from the three inverter legs. Eq. (7) shows the shaft voltage of the motor. Eq. (8) is another form of (7). Eq. (9) shows the shaft voltage about magnetic flux density on the shaft [7, 8].

$$V_{com} = \frac{V_{ao} + V_{bo} + V_{co}}{3} \tag{6}$$

$$\frac{1}{C_r}\frac{d(V_{sh} - V_{com})}{dt} + \left(\frac{1}{C_B} + \frac{1}{C_g} + \frac{1}{C_{mg}}\right)\frac{d(V_{sh})}{dt} = 0 \tag{7}$$

$$V_{sh1} = \frac{C_r}{C_r + C_B + C_g + C_{mg}} \times V_{com} \tag{8}$$

$$V_{sh2} = \frac{d(B_{sh})}{dt} \tag{9}$$

5. Design of Proposed Model

There are many methods to reduce the shaft voltage, but some of these cannot be used in special cases. In such cases, there is no option to suppress shaft voltage by modifying the magnetic and electric circuits. Therefore, we re-designed magnetic circuit of the motor to suppress shaft voltage. From (2)-(9), these design variables mainly affect shaft voltage as shown (10). As shown in Fig. 6, the

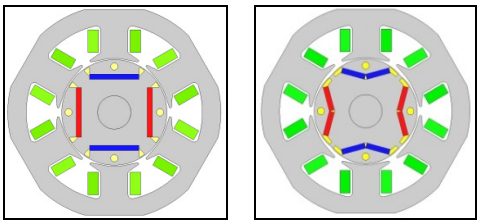

(a) Initial motor (b) Proposed motor

Fig. 6. Initial motor and proposed motor

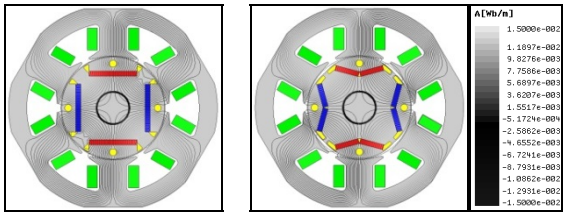

(a) Initial motor (b) Proposed motor

Fig. 7. The linkage magnetic flux line of motors

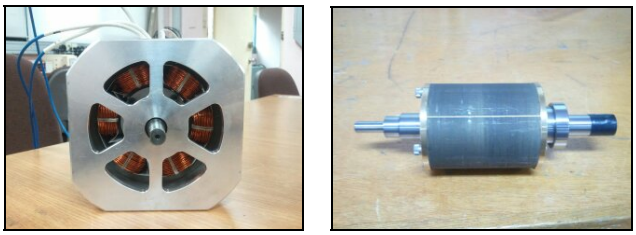

(a) The proposed motor (b) The proposed rotor

Fig. 8. The proposed motor

magnet shape is changed from the initial motor to a proposed motor. In the case of the proposed motor, shaft voltage is suppressed by increasing the C_{mg} value and reducing the C_r value. When the C_{mg} value increases, the distance between the magnet and the shaft (d_m) decreases. When the C_r value decreases, the air-gap length of the arc part (g_1) increases. Fig. 7 shows the linkage magnetic flux line of motors. Also, shaft voltage is suppressed by decreasing the linkage magnetic flux on the shaft. Fig. 8 shows the manufactured models [9, 10].

$$\begin{aligned} C_r &= f(g_{arc}), C_{mg} = f(\theta_{PM}) \\ V_{sh} &= f(C_r, C_{mg}) \end{aligned} \tag{10}$$

6. Analysis and Results

Table 1 shows the measurement value and the calculated value by equation. The Calculated shaft voltage is not include the linkage magnetic flux on the shaft. So, the calculated shaft voltage is bigger than the measurement shaft voltage.

The experimental sets, for shaft voltage measurement under a no-load condition are shown in Fig. 9. The typical stray capacitance within the brushless DC motor is between several pF and several hundreds pF, the influence from the stray capacitance to electrostatic capacity in the measurement equipment and in other equipment shall be minimized. The oscilloscope probe input capacitance forms a parallel circuit with the measurement circuit, the shaft voltage may not be measured correctly. Therefore, a differential probe having lower electrostatic capacity is

Table 1. The value of parasitic parameter and shaft voltage

	Initial motor	Proposed motor
C_r	5.46 pF	3.93 pF
C_{mg}	7.52 pF	13.08 pF
V_{sh} (calculation)	4.99 V	3.46 V
V_{sh} (measurement)	4.25 V	2.56 V

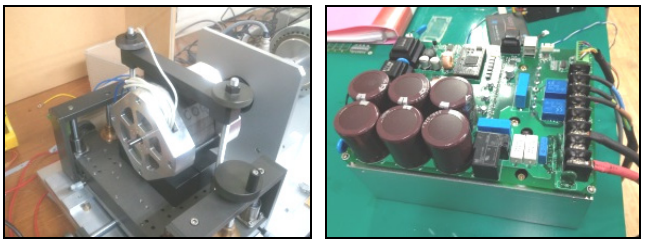

Fig. 9. Equipment setup for the shaft voltage measurement

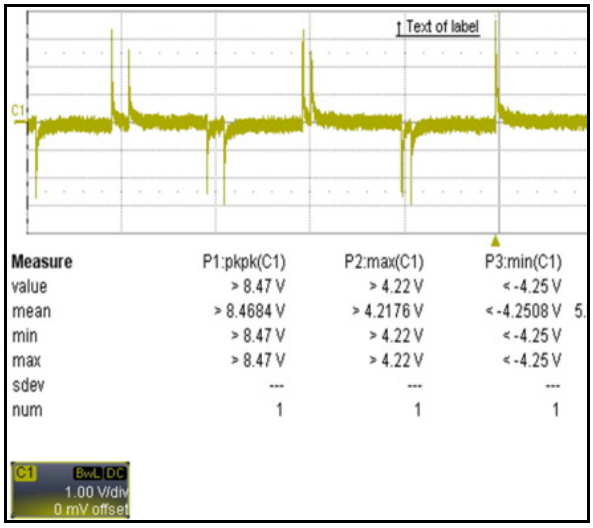

Fig. 10. The shaft voltage of initial motor (10 V/div)

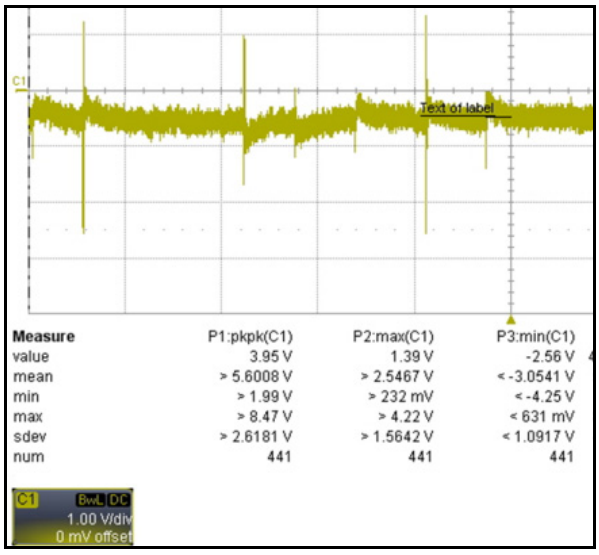

Fig. 11. The shaft voltage of proposed motor (10 V/div)

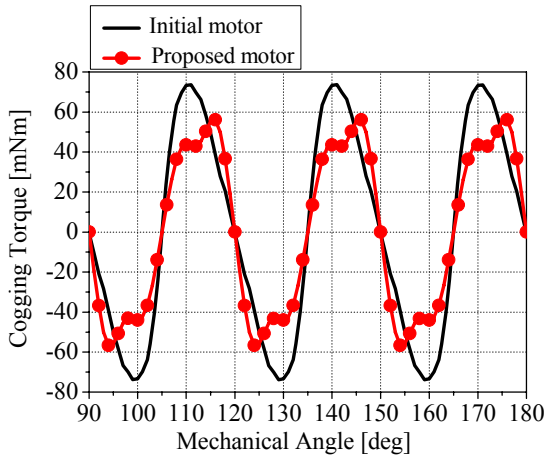

Fig. 12. The cogging torque

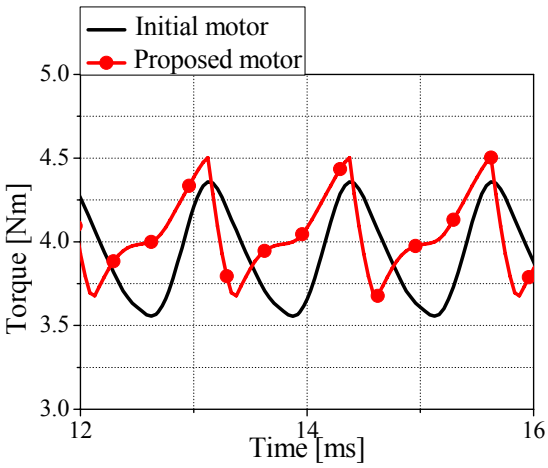

Fig. 13. The commutation torque

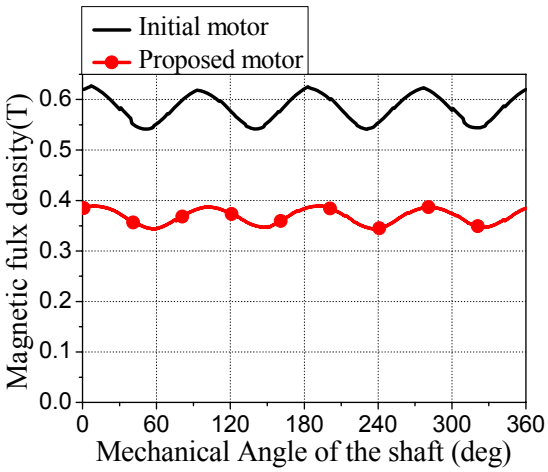

Fig. 14. The magnetic flux density on the shaft

used in the experiment and voltage relative to the metal bracket is measured to obtain the shaft voltage [4]. Fig. 10, 11 show the experimental results for the shaft voltage of the initial and the proposed motor. The shaft voltage of the

proposed motor is lower than the shaft voltage of initial model. Shaft voltage of the proposed model is 2.56 [V]. It was reduced 39% than initial model because the magnet and rotor shape change. Fig. 12 shows the cogging torques. The shaft voltages of the proposed models are lower than for the initial motor. The reduced cogging torque can be checked by an applied arc in the rotor. Fig. 13 shows the commutation torques. The ripple of the commutation torque is reduced by the arc-shaped rotor and V-shaped magnet. Fig. 14 shows the simulation results for the total magnetic flux density of the shaft. The simulation results for the shaft voltage are without the bearing.

7. Conclusions

In this paper, we propose an improved shape for the permanent magnets of IPM-type high-voltage motors to reduce shaft voltage, without affecting torque characteristics. Shaft voltage has become a serious problem in high-voltage motors. If a bearing fault occurs, the industrial production will be stopped. In the case of the proposed motor, shaft voltage is suppressed by increasing the C_{mg} value and reducing the C_r value. In addition, shaft voltage is suppressed by reducing the linkage magnetic flux on the shaft. The shaft voltage of the proposed motor is lower than the shaft voltage of initial model. Shaft voltage of the proposed model is 2.56 [V]. It was reduced 39% than initial model because the magnet and rotor shape change. Therefore, we can expect an increase in operation time due to the increased efficiency and reduced shaft voltage.

Acknowledgements

This work was supported by the Energy Efficiency & Resources of the Korea Institute of Energy Technology Evaluation and Planning (KETEP) grant funded by the Korea government Ministry of Science, ICT & Future Planning (No. 2012T100201723) and the MSIP (Ministry of Science, ICT & Future Planning), Korea, under the CITRC (Convergence Information Technology Research Center) support program (NIPA-2013-H0401-13-1008) supervised by the NIPA(National IT Industry Promotion Agency)

References

[1] H. William Oh and A. Willwerth, "Shaft grounding-a solution to motor bearing currents," *Refrigerating and Air-Conditioning Engineers, Inc. Published in ASHRAE Transactions*, Vol. 114, No. 2, 2008.

[2] T. Maetani, S. Morimoto, K. Iimori, Y. Isomura, and A. Watanabe, "Approaches to suppressing shaft voltage in brushless DC motor driven by PWM inverter," *presented at 2011 Int. Conf. Elect. Mach. Syst. (ICEMS)*, pp. 1-6.

[3] J. Adabi, F. Zare, G. Ledwich, A. Ghosh, and R. D. Lorenz, "Bearing damage analysis by calculation of capacitive coupling between inner and outer races of a ball bearing," *presented at the Conf. Power Electronics and Motion Control.*, pp. 903-907, Sept. 2008.

[4] J. Adabi, F. Zare, A. Ghosh, and R.D. Lorenz, "Calculations of capacitive couplings in induction generators to analyse shaft voltage," *IET Power Electron.*, Vol. 3, No. 3, pp. 379-390, 2010.

[5] A. Muetze and A. Binder, "Calculation of influence of insulated bearings and insulated inner bearing seats on circulating bearing currents in machines of inverter-based drive systems," *IEEE Trans. Ind. Appl.*, Vol. 42, No. 4, pp. 965-972, 2006.

[6] A. Muetze, and A. Binder, "Techniques for measurement of parameters related to inverter-induced bearing currents," *IEEE Trans. Ind. Appl.*, Vol. 43, No. 5, pp. 1068-1074, 2007.

[7] Nho-Van Nguyen, Hai-Thanh Quach, and Hong-Hee Lee, "Novel Single-state PWM Technique for Common-Mode Voltage Elimination in Multilevel Inverters," *JPE*, Vol. 11, No. 4, pp. 548-558, 2012.

[8] Mohd Junaidi Abdul Aziz, Christian Klumpner, and Jon Clare, "Common Mode Voltage Cancellation in a Buck-Type Active Front-End Rectifier Topology," *JPE*, Vol. 12, No. 2, pp. 276-284, 2012.

[9] G. H. Kang, Y. D. Son, G. T. Kim, and J. Hur, "The novel cogging torque reduction method for interior type permanent magnet motor," *IEEE Trans. Ind. Appl.*, Vol. 45, pp. 161-167, Jan. 2009.

[10] G. H. Kang, J. Hur, B. W. Kim and B. K. Lee, "The shape design of interior type permanent magnet BLDC motor for minimization of mechanical vibration," *IEEE Conf. Energy Convers.*, pp. 2409-2414, Sep. 2009.

Kyung-Tae Kim was born in Busan, Korea. He received his B.S. and M.S. in Electrical Engineering from the University of Ulsan, Ulsan, Korea, in 2010 and 2012, respectively. Since 2012, he has been working towards his Ph.D. at the University of Ulsan. His current research interests include motor design and motor diagnosis.

Sang-Hoon Cha was born in Ulsan, Korea, in 1984. He received the B.S. and the M.S. degrees in electrical engineering from the University of Ulsan, Ulsan, Korea, in 2011 and 2013, Since 2013, he is researcher in Korea Marine Equipment Research Institute. His research interests are in the areas of motor design, suppression of shaft voltage.

Jin Hur (S'93-M'98-SM'03) received his Ph.D. in Electrical Engineering from Hanyang University, Seoul, Korea, in 1999. From 1999 to 2000, he was with the Department of Electric Engineering, Texas A&M University, College Station, TX, as a Postdoctoral Research Associate. From 2000 to 2001, he was a Research Professor of Electrical Engineering for BK21 projects at Hanyang University. From 2002 to 2007, he was a Director of Intelligent Mechatronics Research Center, Korea Electronics Technology Institute (KETI), Puchon, Korea, where he worked on the development of special electric machines and systems. Since 2008, he has been an Associate Professor, School of Electric Engineering, University of Ulsan, Ulsan, Korea. He is the author of over 140 publications on electric machine design and control. He has 1 granted pending US patent and 20 granted pending Korean patents. His current research interests include high-performance electrical machines and fault diagnosis. Dr. Hur is working as an Associate Editor for IEEE Transaction on Power. He is also an IEEE Senior Member.

Jae-Sun Shim received his B.S. and Ph.D. degree in Electrical Engineering from Sungkyunkwan University, Suwon, Korea, in 1973 and 1989, respectively, and his M.S. in Electrical Engineering from Dankook University, Seoul, Korea, in 1979. He has been with Kang won National University at Samcheok, Korea, as professor in the Department of Electrical Engineering since 1975.

Byeong-Woo Kim received his B.S. and M.S. in Mechanical Engineering from Hanyang University, Seoul, Korea, in 1987 and 1990, respectively and his Ph.D. in Precision Mechanical Engineering from Hanyang University, in 2002. From 1989 to 1990, he was an Invited Researcher at the Precision Measurement Group, Japan Kosaka Research Institute, Saitama, Japan. From 1990 to 1994, he was a Junior Researcher at the Sensor Development Group, CAS Cooperation, Seoul, Korea. From 1994 to 2006, he was a Principal Researcher at the Electrical & Electronics Group, Korea Automotive Technology Institute, Chunan, Korea. In 2006 Dr. Kim joined the School of Electrical, Electronics and Information Systems Engineering, Ulsan University, Ulsan, Korea, as an Associate Professor. His current research interests include electrical and electronics systems for automotive applications, and control systems for hybrid, fuel cell and electric vehicle systems.